

NO-8884 888

AIR FORCE GEOPHYSICS LAB HANSCOM AFB MA
MAGNETIC DISTURBANCE STATISTICS FROM A SINGLE STATION @ INDEX A--ETC(U)
DEC 79 B S DANDEKAR
AFGL-TR-79-0296

F/O 17/9

UNCLASSIFIED

NL

[OF]
20A
004808



END

7-89

hV

12

AFGL-TR-79-0296
ENVIRONMENTAL RESEARCH PAPERS, NO. 687



LEVEL II

**Magnetic Disturbance Statistics
From a Single Station Q Index
Applied to an Actual OTH-B Radar Situation**

B. S. DANDEKAR

DTIC
ELECTRONIC
MAY 30 1980
C

18 December 1979

Approved for public release; distribution unlimited.

DDC FILE COPY

SPACE PHYSICS DIVISION PROJECT 4643
AIR FORCE GEOPHYSICS LABORATORY
HANSCOM AFB, MASSACHUSETTS 01731

AIR FORCE SYSTEMS COMMAND, USAF

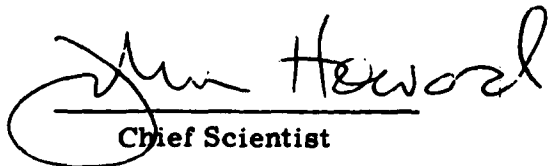


80 5 28 006

This report has been reviewed by the ESD Information Office (OI) and is releasable to the National Technical Information Service (NTIS).

This technical report has been reviewed and is approved for publication.

FOR THE COMMANDER


Chief Scientist

Qualified requestors may obtain additional copies from the Defense Documentation Center. All others should apply to the National Technical Information Service.

Unclassified

SECURITY CLASSIFICATION OF THIS PAGE (When Data Entered)

REPORT DOCUMENTATION PAGE		READ INSTRUCTIONS BEFORE COMPLETING FORM
1. REPORT NUMBER AFGL-TR-79-0296	2. GOVT ACCESSION NO. AD-A084 808	3. RECIPIENT'S CATALOG NUMBER
4. TITLE (and Subtitle) MAGNETIC DISTURBANCE STATISTICS FROM A SINGLE STATION Q INDEX APPLIED TO AN ACTUAL OTH-B RADAR SITUATION		5. TYPE OF REPORT & PERIOD COVERED Scientific. Interim.
7. AUTHOR(s) B. S. Dandekar		6. PERFORMING ORG. REPORT NUMBER FRP No. 687
9. PERFORMING ORGANIZATION NAME AND ADDRESS Air Force Geophysics Laboratory (PHI) Hanscom AFB Massachusetts 01731		8. CONTRACT OR GRANT NUMBER(s)
11. CONTROLLING OFFICE NAME AND ADDRESS Air Force Geophysics Laboratory (PHI) Hanscom AFB Massachusetts 01731		10. PROGRAM ELEMENT, PROJECT, TASK AREA & WORK UNIT NUMBER 62101F 46430609
14. MONITORING AGENCY NAME & ADDRESS (if different from Controlling Office)		12. REPORT DATE 18 December 1979
		13. NUMBER OF PAGES 40
		15. SECURITY CLASS. of this report Unclassified
		15a. DECLASSIFICATION/DOWNGRADING SCHEDULE
16. DISTRIBUTION STATEMENT (of this Report) Approved for public release; distribution unlimited.		
17. DISTRIBUTION STATEMENT (of the abstract entered in Block 20, if different from Report)		
18. SUPPLEMENTARY NOTES		
19. KEY WORDS (Continue on reverse side if necessary and identify by block number) Magnetic activity index Auroral oval Auroral ionospheric disturbance		
20. ABSTRACT (Continue on reverse side if necessary and identify by block number) Due to the systematic diurnal motion of the auroral oval, the Q values of magnetic activity derived from a single station are not directly usable to determine the expected degree of auroral activity. To remove the diurnal effects from a single station data base, which leads in daytime to an under-estimation of the Q index, an empirical set of detrending factors was determined for the Sodankyla Q data base. These factors show that the probability that a given level of magnetic activity will be exceeded for a given duration is underestimated by up to a factor of 2 in the least sensitive daytime sector.		

DD FORM 1 JAN 73 1473

Unclassified

SECURITY CLASSIFICATION OF THIS PAGE (When Data Entered)

Unclassified

SECURITY CLASSIFICATION OF THIS PAGE(When Data Entered)

20. (Cont)

The detrended data base has been analyzed to determine the probability that a given Q value is exceeded for a selected duration. This analysis has been done for durations up to 12 hr separately for the night and daytime detrended data bases. The results are very similar and confirm that the detrending has been successfully accomplished. Finally the individual and cumulative probabilities that a given Q is exceeded for a selected duration (periods from 0.25 to 24 hr) have been established for the fully detrended data base. To interpret the results in their effect on the Over-the-Horizon Experimental Radar System, the distribution of probabilities has been modulated with the dynamics of the auroral oval by use of the Starkov equation (1969). This permits the assessments of the probability that a fixed location in the radar coverage area is under the auroral oval.

For determining the durations of auroral disturbances at various corrected geomagnetic latitudes within any test area under surveillance, a number of tables and figures are presented to explain the procedure.

For the convenience of a user, a series of graphs are included in the report. These graphs present the probability of auroral disturbances of various durations at different latitudes in the Experimental Radar System (ERS) test area.

Unclassified

SECURITY CLASSIFICATION OF THIS PAGE(When Data Entered)

Preface

The author thanks J. Buchau, G. Sales, and A. L. Snyder for their interest in the work, and to World Data Center, Boulder, Colorado for providing the data for the Q index.

Accession For	
NTIS GINA	<input checked="checked" type="checkbox"/>
DDC TAB	<input type="checkbox"/>
Unannounced	<input type="checkbox"/>
Justification	
By _____	
Distribution/	
Availability Code	
Dist	Availability of Special
A	

Contents

1. INTRODUCTION	7
2. ANALYSIS AND INTERPRETATION	8
3. DETERMINATION OF THE IMPACT OF MAGNETIC DISTURBANCES ON THE REGION COVERED IN THE TESTS OF THE OTH RADAR SYSTEM	18
4. CONCLUSIONS	39

Illustrations

1. Percent of Time That Observed $Q \leq$ Ordinate is in 15-min Intervals	8
2. Highest Observed Q Value in 15-min Intervals for the Years 1965, 1969, 1971, and 1974 Respectively	10
3. Factors for Detrending the Observed Q Index Data	12
4. Diurnal Variation of the Q Index From Sodankyla (Year 1974)	14
5. Seasonal Variation of the Q Index From Sodankyla (Year 1974)	14
6. Coverage Area of the OTH-B ERS System in Geomagnetic Coordinates	19
7. Percent Obscuration of the OTH-B ERS Coverage Area Due to Auroral Disturbances in 1974 as Determined From Sodankyla Detrended Q Index	23
8. Time Coverage at Different Corrected Geomagnetic Latitudes of the ERS Test Area	28

Illustrations

9.	The Diurnal Latitude Dependence of the Auroral Oval for Various Q Values	24
10-1 through 10-18.	Probabilities for Various Durations at a Given CG Latitude and a Single CG Longitude of the ERS Test Area	31-35
11a1.	Copy of Figure 10-8.	37
11a2.	Copy of Figure 10-13	37
11b1.	Probability That the Entire ERS Test Area at $\lambda = 65^\circ$ Would be Affected by the Auroral Oval	37
11b2.	Similar to That of Figure 11b1 for $\lambda = 72^\circ$	37
11c1.	Probability That Any Point in the ERS Test Area at $\lambda = 65^\circ$ Would be Affected By the Auroral Oval	38
11c2.	Similar to That of Figure 11c1 for $\lambda = 72^\circ$	38

Tables

1.	Empirical Factors for Detrending the Q Index Data From Sodankyla	12
2.	Probability (%) For Being Equal to or Exceeding a Given Q Level for a Given Minimum Duration	16
3.	Percent of a Day That a Point With a Specified CG Latitude λ is Poleward of the Equatorial Oval Boundary, as a Function of Q	21
4.	Probability for the Distribution of the Q Index for Various Years	22
5.	Probability in Percent of a Year That Any Point With a Specified CG Latitude is Under a Disturbance of a <u>Minimum Given</u> Duration, Independent of Longitude (from Year 1974)	25
6.	Probability in Percent of a Year That a Point on Narssarssuaq Longitude, With Specified CG Latitude is Under Disturbance of a <u>Minimum Given</u> Duration	27

Magnetic Disturbance Statistics From a Single Station Q Index Applied to an Actual OTH-B Radar Situation

1. INTRODUCTION

In a preliminary study, the magnetic activity index Q (observed from a single ground station, Sodankyla, geographic coordinates 67.4°N , 26.6°E ; corrected geomagnetic coordinates 63.4°N , 108.9°E) was used to determine the duration of various levels of magnetically disturbed periods. It was noticed that the Q index measured from a single station, which moves in and out of the auroral oval due to the rotation of the earth, shows a strong diurnal variation. This report attempts to eliminate the diurnal trend from the data and presents the corrected statistics of the durations of the disturbed periods. This analysis is based on the Q index data for the year 1974 that showed the largest magnetic disturbances during the 20th solar cycle.

In the second half of this report, the statistics of the duration of the disturbed periods and the analytical presentation of the auroral oval are combined to determine the impact of the aurora on the geographical area of the OTH-B Experimental Radar System (ERS).

(Received for publication 18 December 1979)

2. ANALYSIS AND INTERPRETATION

To determine a process for the elimination of the diurnal variation of the Q index from a single station (Sodankyla), it is necessary to understand the cause and the extent of the diurnal variation. For this purpose the decile curves for the 1974 Q-index data are presented in Figure 1. The abscissa shows the time in UT and the ordinate shows the Q index. The ordinate scales of the curves are staggered to avoid the mixing of the decile curves. A look at the figure reveals that all the curves show a systematic minimum between 06-10 UT and a maximum between 20-02 UT. Combining the auroral dynamics with the geographical location of Sodankyla, results in the maximum distance between the oval and the station at 09 UT and the minimum distance at 23 UT. These timings match with the timings of the minimum and of the maximum in the diurnal variation of the Q index. Additional proof is the behavior of the top percentile (100 percent), that includes the highest values of the Q index. The highest values refer to severe magnetic disturbances. One would expect these to occur randomly and thus be uniformly distributed over the time scale. As shown in Figure 1, the Q index never exceeded the value of 5 in the time interval 0730-0915 UT, whereas it attained the levels 8 or 9 in the time intervals 1900-0500 UT.

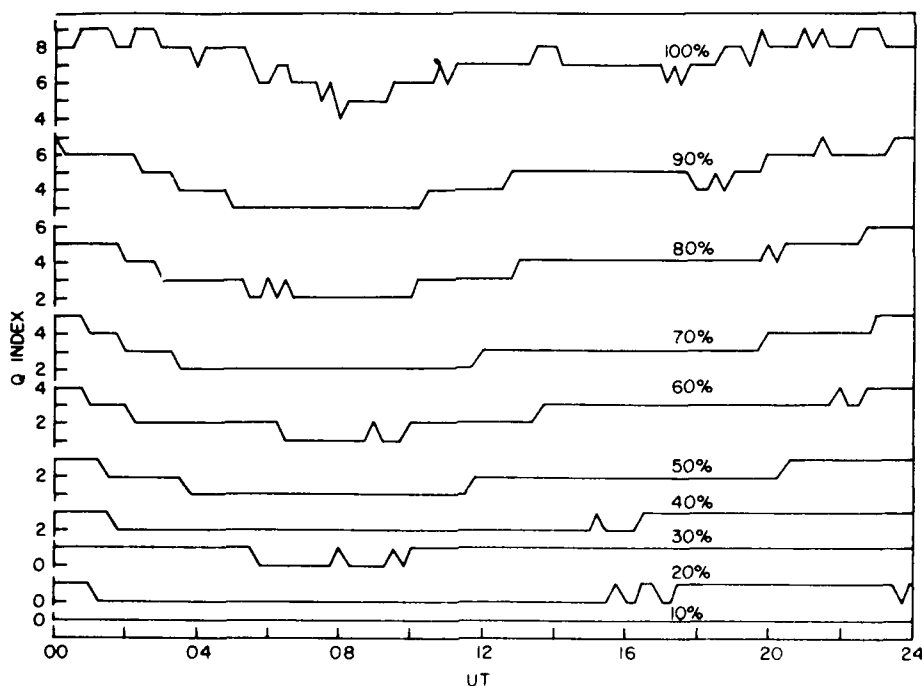


Figure 1. Percent of Time That Observed Q \leq Ordinate is in 15-min Intervals

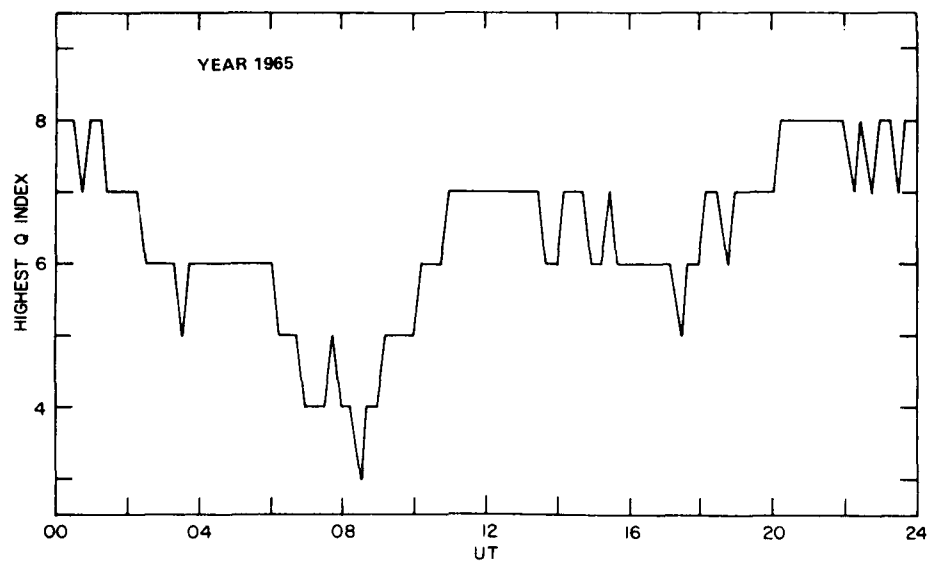
Thus, even during the most severe global disturbances, the diurnal oval motion modulates the observed level of disturbance showing that Q is truly an auroral parameter.

The distribution of the observed Q values for 1974 is similar for all phases of the solar cycle. The fact is seen in the 100 percentile curves for 1965, 1969, 1971 and (1974 for completeness) again 1974 (Figures 2a to 2d). However the maximum level of Q=9 is never observed during 1965, the year of minimum activity in the previous (20th) solar cycle. Also the highest values of Q observed during the quietest time of the day (Q=3 at 0815 UT) are lower than for any other year of the solar cycle. The most enhanced distribution of Q is found in 1974, about three years after 1971, the year of maximum solar activity.

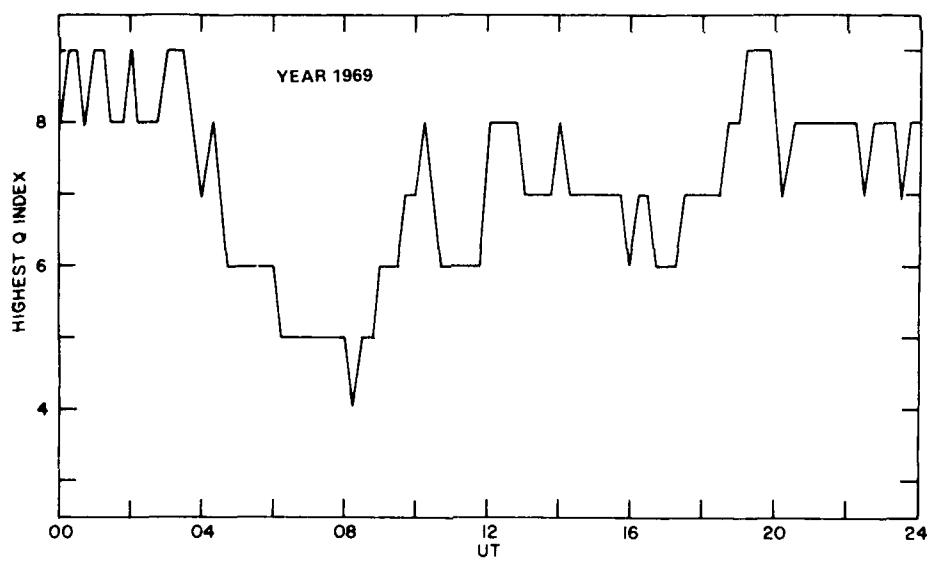
The described distribution of the 100 percentile curve of Q with a minimum around local magnetic midnight was first noticed by Bartels and Fukushima,¹ who initially suggested the method of determining the Q index from D, and H observations of magnetic components from auroral stations.

Thus, one can visualize a correction factor, dependent upon the distance between the locations of the oval and the station, for the elimination of the diurnal variation of the Q index. In determining the factor, several items have to be considered. The Q index has a range from 0 to 9 (also I and F, Ten and Eleven respectively), and an unequal distribution with 60 percent of the values in the range of 8 ± 2 . Thus a simple arithmetical average would not be appropriate. To overcome the difficulty of eliminating the daily trend in the distribution of the Q index, a ratio is determined from each percentile curve by dividing the highest value of the percentile by the corresponding 15-min value of that percentile. Percentile curves with Q=0 are not used. Thus referring to Figure 1, of the ten curves, the top seven with nonzero Q are used. The effect of not incorporating the lowest three decile curves into the detrending process is small, since the 10 percentile has no diurnal variation and for the 20 and 30 percentiles the diurnal variation is only one Q level. In comparison the diurnal Q level ranges for the higher percentiles are ΔQ : 1, 2, 3, 3, 4, 4 and 5 levels for the 40 to 100 percentile curves respectively. From these factors an average factor for each 15-min interval is computed for that year. The study shows that the factors for each year do not show any obvious dependence on the phase of the solar cycle. Therefore for eliminating the solar cycle dependence if any, factors are averaged from the data for the four years 1965, 1969, 1971, and 1974. The final factors are plotted in Figure 3 and are summarized in Table 1.

1. Bartels, J., and Fukushima, N. (1956) Ein Q-index für die ird magnetische aktivität in viertestündlichen intervallen, Abhandl. Akad. Wiss. Göttingen, Math.-Phys. Klasse, Sonderheft-2.

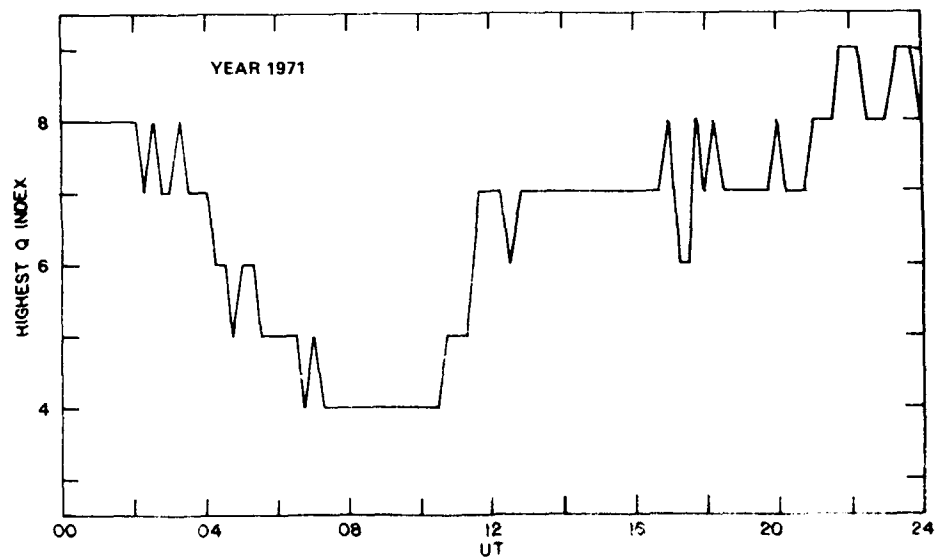


2a

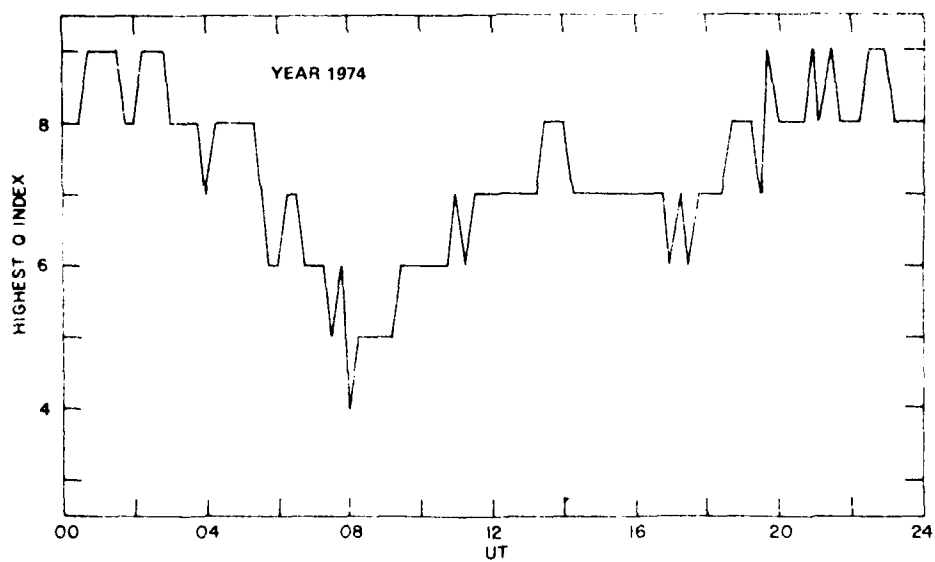


2b

Figure 2. Highest Observed Q Value in 15-min Intervals for the Years 1965, 1969, 1971, and 1974 Respectively



2c



2d

Figure 2. Highest Observed Q Value in 15-min Intervals for the Years 1965, 1969, 1971, and 1974 Respectively (Cont)

Table 1. Empirical Factors for Detrending the Q Index Data From Sodankyla

Hour (UT)	Quarterly Intervals of the Hour				Hour	Quarterly Intervals of the Hour			
	1	2	3	4		1	2	3	4
0	1.0	1.1	1.1	1.1	12	1.7	1.7	1.6	1.6
1	1.1	1.2	1.3	1.3	13	1.6	1.6	1.5	1.5
2	1.4	1.4	1.5	1.6	14	1.5	1.5	1.5	1.5
3	1.6	1.7	1.8	1.9	15	1.4	1.4	1.4	1.4
4	1.9	1.9	2.0	2.0	16	1.4	1.4	1.4	1.4
5	2.1	2.2	2.2	2.2	17	1.4	1.4	1.3	1.3
6	2.3	2.3	2.4	2.5	18	1.3	1.3	1.3	1.3
7	2.5	2.5	2.5	2.5	19	1.3	1.3	1.3	1.3
8	2.6	2.6	2.6	2.5	20	1.2	1.2	1.2	1.2
9	2.5	2.5	2.4	2.3	21	1.1	1.1	1.1	1.1
10	2.2	2.1	2.1	2.0	22	1.0	1.0	1.0	1.0
11	2.0	1.9	1.8	1.7	23	1.0	1.0	1.0	1.0

Multiply the observed Q from Sodankyla by the respective factor from the table for detrending the diurnal variation

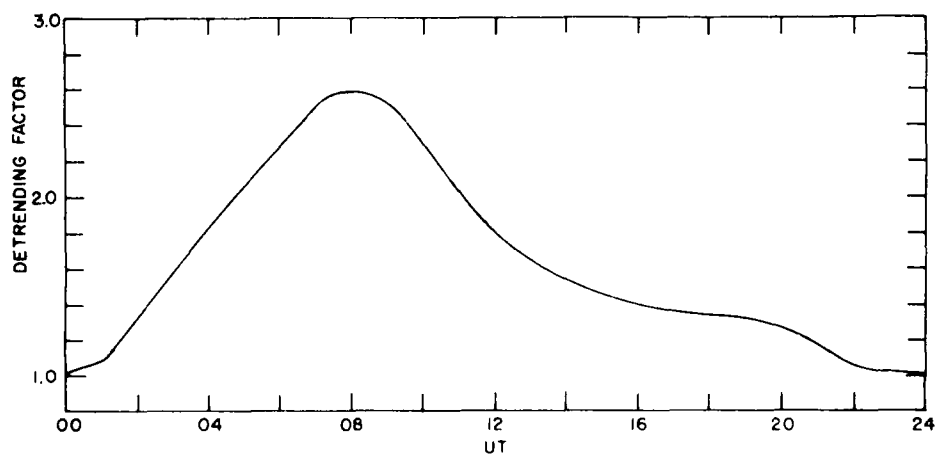


Figure 3. Factors for Detrending the Observed Q Index Data

The detrending factors for each 15-min interval are plotted in Figure 3. The abscissa shows the time of observation in UT and the ordinate presents the factor for correcting the observed Q value for the diurnal and solar cycle dependence. Figure 3 shows that during the afternoon and nighttime, the factors range between 1.0 and 1.5 but the factors exceed 2.0 for a 6-hr time interval centered on 08 UT.

In the following, we will investigate how well the detrending factors in Figure 3 eliminate the diurnal bias from the observed data base. The factors are presented in Table 1 so as to be easily available for use.

In using these factors it should be noted that: (a) the observed values of the Q index are integers ranging from 0-9 (scale extends up to 11); when multiplied, some values may exceed the range; and (b) the factor will not change the observations with $Q=0$.

This second shortcoming can be partially overcome by replacing the observed value $Q=0$ by $Q=0.25$ and rounding the value after the multiplication with the respective factor. This brings in a dilemma. Only in the range of 05-11 UT (factor ≥ 2.0) will this correction have an effect on original $Q=0$ that the corrected Q in this time interval will invariably be 1. However the replacement ($Q=0.25$) will not affect the original values of $Q=0$ in the time interval 11-05 UT. The overall effect in such replacement $Q=0.25$, will be that the very mildly disturbed conditions, with corrected $Q=1$ in the interval 05-11 UT will be slightly overemphasized.

In view of the dilemma that retaining $Q=0$ leads to an underestimation and the replacement of $Q=0$ by $Q=0.25$ results in slight overestimation, and in both cases to a small distortion of the Q distribution for quiet conditions, $Q=0.25$ has been chosen.

The effect of applying the factors to correct the diurnal variation in 1974 is shown in Figure 4. In the figure, the abscissa is the time in UT and the ordinate presents the Q index. The continuous curves show the uncorrected values. The lower curve is for the average value and the upper curve is the average plus one standard deviation. The corresponding detrended curves are shown by the dashed lines. The diurnal variation of the uncorrected average Q index ranges from 1.2 to 3.2. The averages determined from the adjusted values range from 3.0 to 3.2. For the top curve (average + σ) the range for uncorrected Q is from 2.2 to 5.6. The adjusted (average curve + σ) ranges from 5.3 to 6.2. Thus the application of the correction factors significantly reduces the range of the diurnal variation.

The reduction in the diurnal variation should also be evident in the seasonal variation of the Q index. The seasonal variation for 09 UT (minimum) and 23 UT (maximum) in the diurnal variation of uncorrected values and detrended values is shown for the year 1974 in Figure 5.

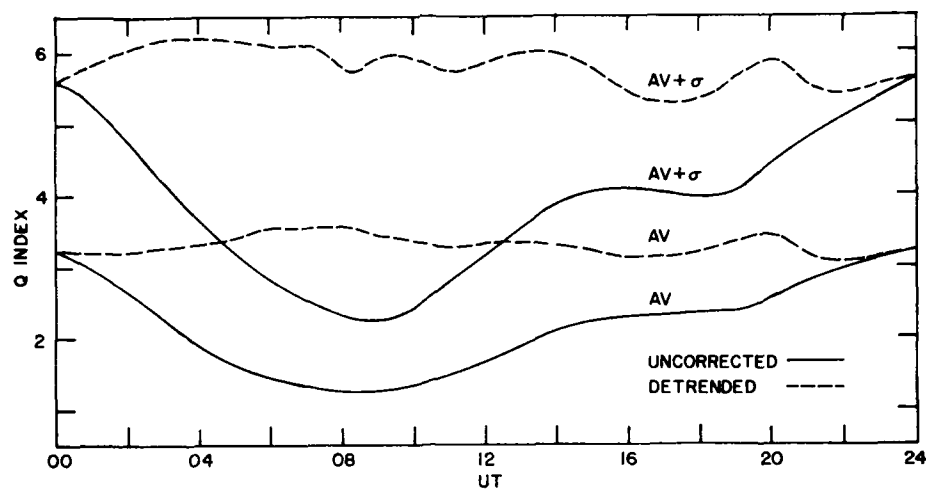


Figure 4. Diurnal Variation of the Q Index From Sodankyla (Year 1974). Continuous curves are for uncorrected data. Dashed curves are for the detrended data

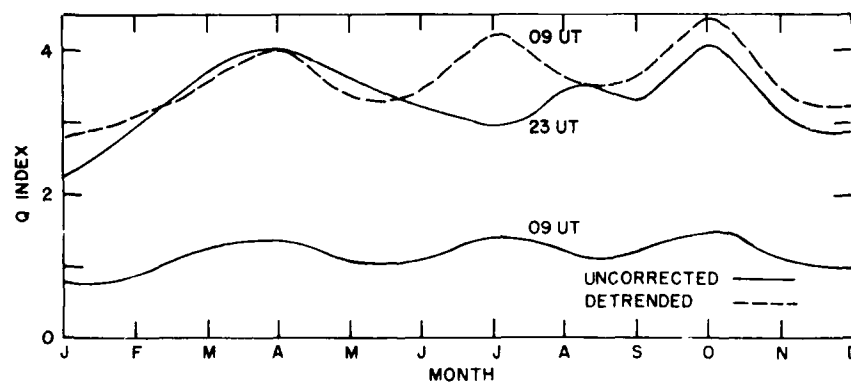


Figure 5. Seasonal Variation of the Q Index From Sodankyla (Year 1974). Continuous curves are for the uncorrected data. Dashed curves are for the detrended data

In Figure 5, the lower continuous curve shows the seasonal variation of the observed uncorrected Q values for 09 UT. The upper continuous curve shows the variation for 23 UT. The difference between the curves is minimum, $\Delta Q \approx 1.5$ in

July and maximum, $\Delta Q=2.6$ in April. When the observed Q values are adjusted by using the factors (from Table 1), the curve for 23 hr UT is unaffected, since this hour provided the reference values for the detrending factors. The adjusted curve of 09 UT, in dashes, lies now close to the curve of 23 UT with largest $\Delta Q=1.3$ in the month of July. For all other months ΔQ is less than 0.5. Again the factors reduce the diurnal variation in the observed uncorrected data for all the seasons.

Due to the systematic minimum in the diurnal variation in the observed values of the Q index (uncorrected data), the duration of a disturbance, exceeding a given Q value based on the original data, will be underestimated. In fact this is seen by dividing the data in two 12-hr intervals, one around the period of the minimum (0130-1330 UT) and the other around the period of the maximum (1330-0130 UT) of the diurnal variation. These results are presented in Table 2, from the data of 1971.

Tables 2a to 2f present the probabilities for the magnetic activity to exceed the levels of Q from 0-8. In each table the top line describes the selection of the data base, nighttime only, daytime only, or all the data. Tables 2a to 2c are derived from the uncorrected data and Tables 2e to 2f are from the data detrended by the factors in Table 1. The column on the left-hand side presents the level of the disturbance equal to or greater than the given Q value. There are 25 columns, each refers to the minimum duration for the disturbance for the Q level defined in the left-most column. Thus the first column presents all durations for a given Q level, whereas the last column on the right-hand side is for durations exceeding one day (24 hours). The probability for the occurrence is presented as a percent of the year. The top line for each section is 100 percent for $Q \geq 0$. This line, though an obvious result, is added for the sake of consistency, and is needed in future computations.

In determining durations from day or nighttime data the succeeding selected (day/night) periods are treated as continuous. This continuity enables the determination of the probability of durations longer than 12 hr (up to 24 hr).

In general in a given table the probability decreases as the duration of disturbance is increased (along a given row). Also for a given duration the probability decreases as the Q level of the disturbance is increased (down a given column).

A comparison of probabilities in Tables 2a and 2b shows that the corresponding probabilities at nighttime are larger than those at daytime. The nighttime probabilities from raw data (Table 2a), show no significant differences, from those from the detrended data (Table 2b) as anticipated in the study of Table 1. The probabilities for the daytime and those for the combined day and night (all data base) show larger changes (Tables 2b and 2c and 2c and 2d). Another interesting feature is that the corrected (all data) probabilities (Table 2e) are about double of those uncorrected nighttime probabilities (Table 2a). Thus, on the whole, not correcting for the systematic diurnal variation of the observations results in a severe underestimation of the real probability.

Table 2. Probability (%) For Being Equal to or Exceeding a Given Q Level for a Given Minimum Duration. Sections a, b, and c refer to uncorrected data. Sections d, e, and f are from detrended data. Sections a and d are for night only; b and e are for day only; c and f use all the data

Q :	Duration Greater Than (Hours)																								
	0	1	2	3	4	5	6	7	8	9	10	11	12	13	14	15	16	17	18	19	20	21	22	23	24
(a) Night Only																									
0	100	100	100	100	100	100	100	100	100	100	100	100	100	100	100	100	100	100	100	100	100	100	100	100	100
1	41	40	39	38	36	35	34	32	31	31	30	29	28	28	27	26	25	25	24	24	24	23	22	21	21
2	32	31	28	26	24	22	21	18	17	15	14	12	11	11	11	10	10	9	8	8	7	7	6	5	
3	24	23	20	17	15	13	11	10	8	7	6	6	5	4	3	3	2	2	2	2	2	2	2	1	
4	16	15	12	9	8	7	5	4	3	3	2	2	1	1											
5	10	9	7	5	4	3	2	1	1	1	1														
6	6	5	3	2	1																				
7	2	2	1																						
(b) Day Only																									
0	100	100	100	100	100	100	100	100	100	100	100	100	100	100	100	100	100	100	100	100	100	100	100	100	100
1	36	34	31	30	29	28	27	26	25	24	23	22	21	21	20	20	18	18	18	17	17	16	16	15	
2	23	20	17	15	13	12	10	9	8	7	7	5	5	5	4	4	4	3	3	3	3	2	2	2	
3	13	10	8	6	4	4	3	2	2	2	1	1	1	1	1	1									
4	6	4	3	2	1	1																			
5	3	2	1																						
6	1	1																							
(c) All Data																									
0	100	100	100	100	100	100	100	100	100	100	100	100	100	100	100	100	100	100	100	100	100	100	100	100	100
1	77	74	71	68	66	64	62	59	57	56	54	53	52	51	49	48	47	46	44	43	42	41	40	39	
2	55	51	46	42	38	35	32	29	26	25	23	20	19	18	16	14	13	12	11	11	9	9	8	8	
3	37	33	28	24	20	17	15	13	11	10	9	7	6	5	5	5	4	3	3	2	2	2	2	1	
4	22	19	15	13	10	8	7	5	4	3	2	2	1	1	1	1									
5	13	11	8	6	5	4	2	2	1																
6	7	5	3	2	1																				
7	3	2	1																						
8	1																								

Table 2. (Cont)

Q	Duration Greater Than (hours)																								
	0	1	2	3	4	5	6	7	8	9	10	11	12	13	14	15	16	17	18	19	20	21	22	23	24
(d) Night Only																									
0	100	100	100	100	100	100	100	100	100	100	100	100	100	100	100	100	100	100	100	100	100	100	100	100	100
1	41	40	39	38	36	35	34	32	31	31	30	29	28	28	27	26	25	25	24	24	24	23	22	21	21
2	32	31	28	26	24	22	21	18	17	15	14	12	11	11	11	10	10	9	8	8	7	7	6	5	
3	29	27	25	22	20	18	16	14	13	11	10	9	8	8	7	7	6	5	5	5	5	5	4	4	
4	22	20	17	14	12	10	9	8	7	6	5	5	4	3	3	3	2	2	2	2	2	2	1	1	
5	14	13	10	7	6	5	4	3	3	2	2	2	1	1											
6	10	8	5	4	2	2	1	1																	
7	6	5	3	2	1	1																			
8	3	1																							
9	1																								
(e) Day Only																									
0	100	100	100	100	100	100	100	100	100	100	100	100	100	100	100	100	100	100	100	100	100	100	100	100	100
1	44	43	43	42	42	42	42	36	34	32	31	29	28	28	28	27	26	26	26	26	25	24	24	24	23
2	36	34	31	29	28	27	26	25	24	23	23	22	21	20	19	19	18	18	17	17	17	16	16	15	15
3	26	22	19	17	14	13	11	10	9	8	7	7	6	6	6	5	5	4	4	4	3	3	3	2	2
4	20	17	14	11	10	8	7	6	5	4	4	3	3	3	3	2	2	2	2	2	2	1	1	1	1
5	16	12	10	8	6	5	4	4	3	3	2	2	2	2	2	1	1	1	1	1	1	1	1	1	1
6	10	7	5	4	3	2	2	1	1	1	1	1	1	1											
7	7	5	3	2	2	1	1	1	1																
8	5	3	2	1	1	1																			
9	3	2	1	1	1																				
(f) All Data																									
0	100	100	100	100	100	100	100	100	100	100	100	100	100	100	100	100	100	100	100	100	100	100	100	100	100
1	85	83	82	80	79	77	76	68	65	63	61	59	58	57	56	55	54	54	53	52	51	51	51	50	48
2	68	64	59	56	53	50	47	44	42	40	38	36	36	34	32	31	30	29	28	27	26	24	23	21	19
3	55	50	44	39	35	31	28	26	23	21	20	19	17	15	14	13	13	12	12	11	10	10	9	9	9
4	42	38	32	26	23	20	17	15	14	12	10	9	9	8	8	7	6	6	6	5	5	5	5	5	5
5	30	25	20	16	13	10	9	8	6	5	4	4	4	4	4	3	3	3	3	3	2	2	2	2	2
6	20	16	11	8	6	5	3	3	2	2	1	1	1	1	1	1	1	1	1	1	1	1	1	1	1
7	13	10	6	4	3	2	2	1	1	1	1	1	1	1											
8	8	4	2	2	1	1																			
9	4	2	1	1																					

Another approach of overcoming this difficulty is to supplement observations from one station by those from another station with a similar latitude but with a longitude separation of approximately 180° . The Observatory at College, Alaska (geographic 64.9°N , 212.2°E) satisfies this requirement for the Observatory at Sodankyla (geographic 67.4°N , 26.6°E).

The Q values from College, Alaska are not routinely available. Therefore an effort is in progress to determine the Q index from the College observations of the D and H components. Both approaches, detrending the single station data and complimenting single station data from a second station, will be followed for overcoming the systematic diurnal variation of Q from a single station.

3. DETERMINATION OF THE IMPACT OF MAGNETIC DISTURBANCES ON THE REGION COVERED IN THE TESTS OF THE OTH RADAR SYSTEM

The irregular features of the auroral and subauroral ionosphere, such as the auroral E-layer, auroral E_s , the highly irregular F-layer (FLIZ or F-Layer Irregularity Zone), auroral absorption, the mid-latitude F-layer trough, and the strong gradients at the interfaces of the various ionospheric structures, are all organized by a now well established frame of reference; The auroral oval.² The dynamic behavior of the auroral oval, controlled by the interplanetary magnetic field and geomagnetic activity, is reflected in associated dynamic changes of the location and intensity of the various ionospheric features mentioned above.

The Over-the-Horizon Backscatter Experimental Radar System (OTH-B ERS) presently under construction in Maine will operate in an area covering a part of Greenland, bounded in the east by Iceland, and extending over a large part of the North Atlantic Ocean.

Every night the auroral oval and thus the auroral ionosphere will affect at least half of the ERS coverage area. The coverage area is shown in Figure 6, superimposed on a section of the northern hemisphere, which is plotted in corrected geomagnetic coordinates. This coordinate system is especially useful for the presentation of auroral phenomena such as the auroral oval.

Two positions of the statistical auroral oval² for $Q=3$ are shown in Figure 6. At 02 UT (23 LT/21 CGT in the center of the ERS coverage area) the oval extends the furthest south (64° Corrected Geomagnetic Latitude) and as shown by the location of equatorward border (bold continuous curve) it covers the top (poleward) one-half area of the radar coverage. At 14 UT (11 LT/09 CGT in the center of the coverage area) the night sector of the oval is in the opposite quadrant and the equatorward border of the day sector shown by bold dashed curve now covers only a small section

2. Feldstein, Y. I. (1963) On the morphology of auroral and magnetic disturbances at high latitudes, Geomag. Aeron. 3:183.

of OTH-B FRS surveillance area (72.5° CGL). Referring to Figure 6, it is seen that for any given level of magnetic activity (in this case $Q=3$), the obscuration of the FRS-test area depends on time due to the diurnal motion of the oval.

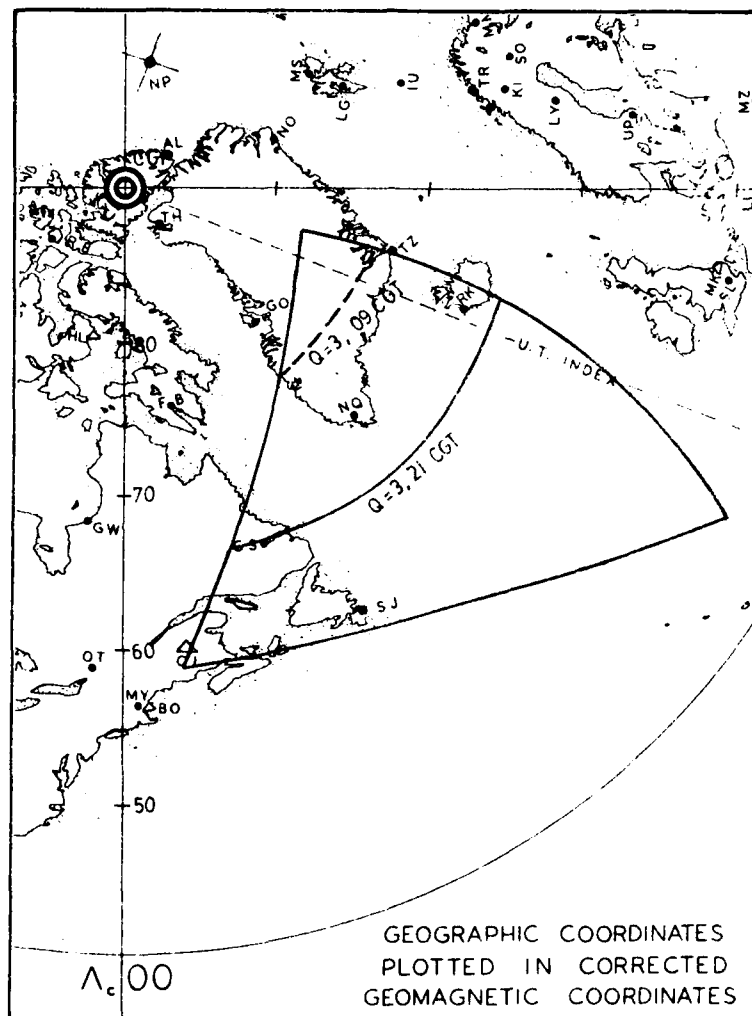


Figure 6. Coverage Area of the OTH-B FRS System in Geomagnetic Coordinates. Note the change in the position of the Q=3 oval at 09 (dashed curve) and 21 CGT (continuous curve)

A given ground station at auroral latitudes, as well as the coverage area of the ERS as a whole, moves underneath and out again from under the oval, each 24-hr period. Due to this diurnal motion, the auroral oval will spread over the varying sections of the coverage area even for a steady Q index (as seen in Q=3 in Figure 6). Additional variation of the area under the auroral oval influence, results from the dependence of the oval diameter on Q. These two variations can be determined in two steps: The variation due to (1) the daily motion of the oval for each Q combined with, (2) the expected variation of the Q index based on measured probabilities.

First we will determine the duration for which the equatorward boundary of the oval will stay equatorward of a given CG latitude for a given Q level of magnetic activity. Since the oval exhibits a 24-hr periodicity the duration is expressed as a percent of a 24-hr period. For this purpose we will use the analytical equation of Starkov³ which describes θ_{eq} , the location of the equatorward boundary of the oval as a function of t, the hour angle, and Q the level of magnetic activity. This equation is based on the study of discrete auroral arcs. The equation is given by

$$\theta_{eq} = 18 + 0.9 Q + 5.1 \cos (t-12^\circ) \quad (1)$$

where

θ is the oval boundary,

Q is the level of magnetic activity on the midnight meridian at 65° CGL, and

t is the hour angle measured in degrees from the midnight meridian eastward towards the morning sector. The equation provides an instantaneous position of the oval, depending on the value of the Q index. The percent of each day, for which a point with a specified CG latitude is under the auroral oval has been determined from Eq. (1). This is done by computing the two values of angle t for a given Q and a given CG latitude from Eq. (1). The difference between the angles divided by 360° provides the fractional period of a day for the given Q and λ . These are presented as a function of Q in Table 3.

The left-hand side column presents the CG latitude of the equatorward boundary of the auroral oval. The Q index levels are shown along the top row. The fractions of 24-hr periods for given Q and λ are presented as percentages along respective rows and columns. For example, if the magnetic activity is continuously at level Q=9, the equatorward boundary would be at or lower than 63° CGL for 0.5 for each day, that is, for 12 hr of each 24-hr period. The latitudes less than 57° are not shown since the statistical oval does not reach such low latitudes. In actuality, on rare occasions the aurora has been observed at latitudes much further south than the 57° CGL predicted from Table 3.

3. Starkov, G. V. (1969) Analytical representation of the equatorial boundary of the oval auroral zone, Geomag. Aeron. (English Edition) 9:614.

Table 3. Percent of a Day That a Point With a Specified CG Latitude λ is Poleward of the Equatorial Oval Boundary, as a Function of Q

	Q Index										
λ	0	1	2	3	4	5	6	7	8	9	10
57											6
58										8	21
59									13	21	29
60								13	23	29	38
61							15	25	31	38	44
62						17	25	33	38	46	50
63					17	25	33	40	46	50	56
64				17	27	33	40	46	50	58	63
65			21	29	33	42	46	52	58	63	71
66	6	21	29	35	42	46	52	58	65	71	79
67	21	29	35	42	48	54	58	65	71	79	94
68	29	38	42	48	54	58	67	71	79	100	100
69	38	42	50	54	60	67	73	83	100	100	100
70	44	50	54	60	67	75	83	100	100	100	100
71	50	54	63	67	75	83	100	100	100	100	100
72	56	63	69	75	85	100	100	100	100	100	100
73	63	71	77	88	100	100	100	100	100	100	100
74	71	79	88	100	100	100	100	100	100	100	100
75	79	92	100	100	100	100	100	100	100	100	100
76	94	100	100	100	100	100	100	100	100	100	100
77	100	100	100	100	100	100	100	100	100	100	100

Table 4a lists the probability that the observed Q would lie in a given interval. Table 4b lists the cumulative probability that the observed Q would be \geq the given value. For the sake of completeness the values are listed for the years 1965, 1969, 1971, and 1974 for the data from Sodankyla. The letter (u) refers to the probabilities from the uncorrected data and (d) refers to those from the detrended data. It is seen that 1974 has the highest values for the probability (Table 4b).

The product of percent period from Table 3 and the probability in Table 4b gives the average percent of time that the auroral oval is equatorward of a given latitude in the coverage area (averaged over the year 1974) for a Q value greater than the selected number.

Based on Tables 3 and 4b the probable average annual duration of coverage by the aurora in percent of time in the OTH-B ERS coverage area is shown in Figure 7. Starting at the lefthand top corner of the coverage area, a very small region shaded is affected all the time. Approximately one-quarter of the area is affected half of the time, whereas the area shaded with lines, which forms one-quarter of the sector in the right-hand bottom corner, is statistically free of any auroral disturbances at all times.

Table 4. Probability for the Distribution of the Q Index for Various Years. (a) Uncorrected and detrended. (b) Cumulative Uncorrected and detrended

(a) Probability (%) for Q to be in a Given Interval								
Q Index	Year							
	1965		1969		1971		1974	
	(u)	(d)	(u)	(d)	(u)	(d)	(u)	(d)
0	62	43	50	36	45	30	23	15
1	19	28	19	24	22	25	22	17
2	9	11	12	12	14	13	18	13
3	5	7	8	10	9	10	15	13
4	2	4	4	7	4	7	9	12
5	1	3	3	5	3	6	6	10
6	1	1	2	3	2	3	4	6
7		1	1	2	1	3	2	6
8				1		2	1	4
9								2
10								1
(b) Cumulative Probability for Q to be \geq the Given Interval								
0	100	100	100	100	100	100	100	100
1	38	57	50	65	55	70	77	85
2	19	28	31	41	34	45	55	68
3	10	18	18	30	19	32	37	55
4	5	11	10	20	10	22	22	42
5	3	6	6	13	6	15	13	30
6	1	3	3	8	3	9	7	20
7		2	1	5	1	6	3	14
8		1		3		3	1	8
9				1		1		4
10				1		1		2

u - Uncorrected, d - Detrended

In Figures 6 and 7, the curves have similar shapes. In Figure 6, the curves present instantaneous positions of the oval (as an example), whereas in Figure 7 the curves present the average percentages of the auroral disturbances, affecting different regions in the test area. As these two figures present entirely different aspects of the effects of Q on the test area, the incidental similarity and/or a match in the shapes of the curves cannot be used for determining the average distribution of the Q index.

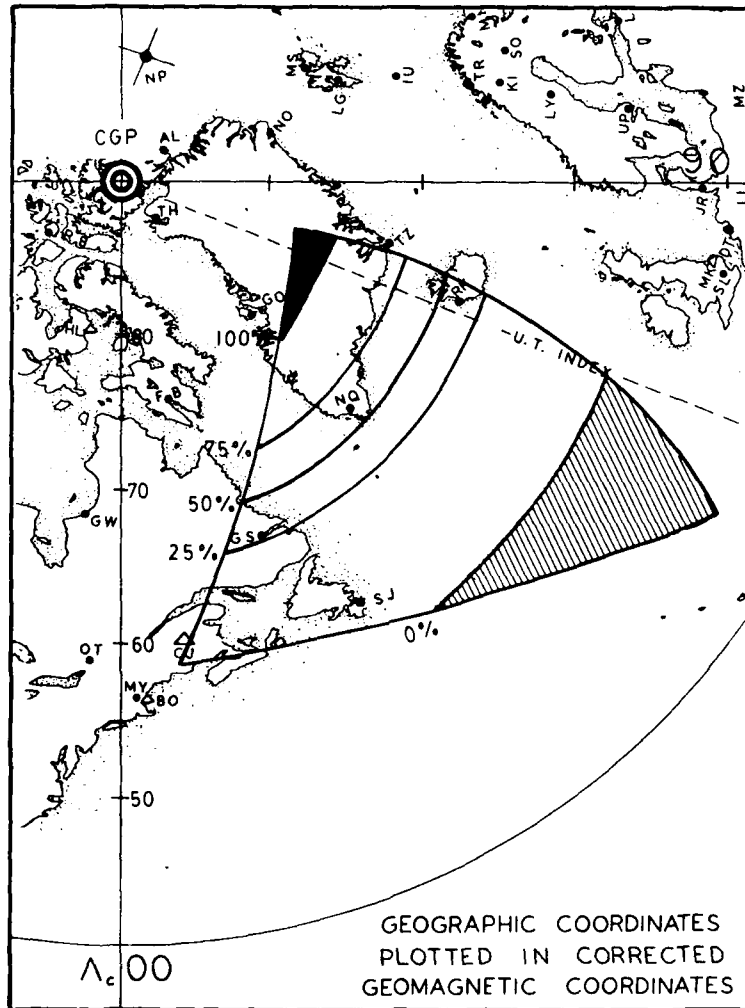


Figure 7. Percent Obscuration of the OTH-B ERS Coverage Due to Auroral Disturbances in 1974 as Determined From Sodankyla Detrended Q Index

In Table 2 we considered the durations of disturbances which depended only on the level of the Q index. Table 3 gives the duration (in percent of a day) that a given point is under the auroral oval, as a function of Q. In order to determine the probability of the duration of a disturbance lasting at a given latitude for a given length of time, these two factors have to be combined. This global probability independent of longitude can be computed from the equation

$$P_{\lambda, d} = \sum P_{\lambda, Q_i} (P_{Q_i, d} - P_{Q_{i+1}, d}) \quad (2)$$

where

$P_{\lambda, d}$ is the probability for duration d at geomagnetic latitude λ ,

P_{λ, Q_i} is the probability for the oval to be at latitude for given Q_i (from Table 3),

$P_{Q_i, d}$ is the probability for the duration d for the given Q index Q_i (from Table 2f),

λ is the CG latitude of a given location,

Q_i is the i th detrended Q index,

i is used for summation over all the values of Q (for $Q \geq 0$, $\sum P_{Q_i, d} = 1.0$).

These probabilities for various lengths of disturbances occurring at different latitudes are listed in Table 5. The lefthand column lists the CG latitude. The top row lists the periods for the duration of the disturbances. For example at 55° CGL durations less than 1 hr have occurrence probability of 1 percent (0.01) whereas at 77° CGL the disturbance is present all the time [1.0 (100 percent)]. This computation does not take into account the longitude of any given location. Essentially the computation converts the (Q, d) domain of Table 2 to the (λ, d) domain on the basis of the Starkov equation. In computing the probabilities with the use of Eq. (2), the respective probabilities from Tables 2f and 3 have to be used as fractions (≤ 1) instead of percentages presented in the tables. For example to compute the probability that a point with $\lambda = 70^\circ$ CGL is under a disturbance of a minimum duration of 12 hr, Eq. (2) uses data for durations of 12 hr (13th column) from Table 2f and data for $\lambda = 70^\circ$ (14th row) from Table 3. The final sum is presented as percent in Table 5 along $\lambda = 70^\circ$ (12th row) and duration of 12 hr (13th column). The result: A probability of 51 percent shows that the equatorward boundary of the oval would be at or below a CG latitude of 70° with a continuous duration of at least 12 hr for 51 percent of the year. This probability is independent of the longitude of a given station. For determining probabilities for a test coverage area, a fixed geographic longitude of the location on the earth, has to be taken into account.

In deriving probabilities listed in Table 5 the durations at various latitudes from Table 3 are used. It is recalled that these durations refer to the maximum available period at a given latitude independent of longitude. In short, it refers to the farthest extent of the oval without restricting or limiting the location to a selected longitude. For example, referring to Eq. (1) for the Starkov auroral circle, the oval is consistently at lower latitudes for longitudes of the night sector and is consistently at higher latitudes for the longitudes which are in the day sector. Therefore, the probabilities in Table 5 really refer to the disturbances affecting the locations on a global scale. In practice, one is restricted to a limited region of a selected longitude sector. That the probabilities in such a case are much smaller (especially when longer durations are considered) is seen in the following approach.

To determine the probabilities of disturbance durations for points along a selected meridian, a direct approach was used. With the use of detrended Q index data of 1974, the latitudinal position of the equatorward oval boundary for each Q value at the Narssarssuaq meridian (NQ in Figure 6) was computed, using the Starkov equation. From this table of boundary locations, the probability distributions of durations of disturbances as a function of CG latitude for various time intervals are computed. These are summarized in Table 6. The format of Table 6 is identical with that of Table 5.

A comparison of the corresponding columns from Tables 5 and 6 shows that the respective magnitudes of probabilities for a global base are larger than those for a single station like Narssarssuaq. The differences are smaller for shorter durations in the columns on the left-hand side of the tables (< 5 percent up to 4 hours). These differences increase progressively from the left-hand side toward the right-hand side of the columns. The differences are very significant for larger durations of disturbances (right-hand side columns). For example at 75° CGI, the probabilities for the disturbances with durations of 3, and 24 hr, on a global base are 94 percent, and 87 percent. The respective values for Narssarssuaq longitude are 91 percent, and 56 percent respectively.

For determining the extent to which the probabilities in Table 6 depend upon longitude, similar tables were computed for the longitudes of stations CAP TOBIN and CARIBOU (TZ and CJ in Figure 6) which lie on the end longitudes defining the sector of the ERS test area. The difference in longitude between these two stations is equivalent to a time difference of 5 hours. The comparison of corresponding values with those in Table 6 produced an excellent agreement (within 3 percent) for 95 percent of these values. Thus one can conclude that the values in Table 6 are reasonably independent of the longitude of the location for durations up to 21 hours.

Table 6. Probability in Percent of a Year That a Point on Narssarsuaq Longitude With Specified CG Latitude is Under Disturbance of a Minimum Given Duration

λ	Duration Greater Than (Hours)																								
	0	1	2	3	4	5	6	7	8	9	10	11	12	13	14	15	16	17	18	19	20	21	22	23	24
59	1																								
60	2	1																							
61	3	3	1																						
62	6	5	3	2	1																				
63	11	9	7	5	4	3	2	1																	
64	16	14	11	9	8	6	4	3	2	1															
65	22	20	18	16	13	12	10	7	6	3	2	1													
66	31	28	26	24	23	21	18	15	13	10	7	4	3	1											
67	38	37	36	35	33	31	29	26	23	19	14	10	7	4	3	1									
68	45	43	42	42	41	41	41	38	33	29	23	18	13	9	5	3	2	1							
69	54	51	50	50	49	49	49	49	45	39	33	27	21	14	8	5	3	2	1						
70	60	58	56	55	55	55	55	55	55	50	44	37	32	24	18	13	9	6	4	3	2	1	1	1	1
71	67	64	62	61	61	61	61	61	61	61	61	61	52	45	39	30	23	16	10	8	5	3	2	2	2
72	74	72	70	69	69	69	69	69	69	69	69	69	63	57	49	42	33	25	18	14	10	8	7	6	6
73	82	80	78	77	77	77	77	77	77	77	77	77	77	77	77	77	64	55	45	38	29	23	19	16	14
74	88	86	85	84	84	84	84	84	84	84	84	84	84	84	84	84	84	74	67	59	50	41	34	28	23
75	94	93	92	91	91	91	91	91	91	91	91	91	91	91	91	91	91	91	91	91	91	91	91	91	91
76	99	99	99	99	99	99	99	99	99	99	99	99	99	99	99	99	99	99	99	99	99	99	99	99	99
77	100	100	100	100	100	100	100	100	100	100	100	100	100	100	100	100	100	100	100	100	100	100	100	100	100

For understanding the relation between the corresponding values of probabilities listed in Tables 5 and 6 one has to consider several factors. One of the considerations is the variation of the (detrended) Q index with various time-spans. The study of the 1974 detrended Q index data from Sodankyla shows that on the average the Q index changes by one unit in the interval of an hour. For all other intervals in the range of 2 to 24 hr, the Q index on the average changes by two units. Referring to the Q index term in the Starkov Eq. (1), it is seen that a unit change in the Q index is equal approximately to 1° change in the latitudinal position of the aurora. Another factor is the diurnal motion of the oval. Again from the Starkov equation one finds that at quiet magnetic conditions, that is, $Q=0$ the oval latitude changes from 77° around local magnetic midnight to 67° around local magnetic noon. Superposed on this is an expansion or a contraction of the oval with the change in the Q index. It would be necessary (but rather difficult) to separate these changes for determining the exact relations in the corresponding values of probabilities in Tables 5 and 6.

Two factors still missing in the above discussion are: (1) a varying time width of the ERS test area at different CG latitudes; and (2) the time (CGLT) dependence of probabilities due to systematic diurnal motion of the auroral oval.

For determining the probability of auroral disturbances over a wide longitude/time zone covered by a test area (like one in Figure 7), one has to consider the length (width) of the window subtended by the sector at each corrected geomagnetic latitude. Effectively it is the angle subtended by each arc of a CG latitude at the CG pole. The measured angles at various CG latitudes in the sector of Figure 7, are presented in Figure 8. In Figure 8, the abscissa is the CG latitude and the ordinate on the left-hand side is the angle subtended by the arc of a CG latitude at the CG pole. The ordinate on the right-hand side of the figure presents the corresponding durations in hours. From Figure 8 it is seen that the time width of the zone is less than 15 min for CG latitudes below 48° and for CG latitudes above 78° . The time width of the sector reaches a maximum of 250 min for latitudes 59° to 61° .

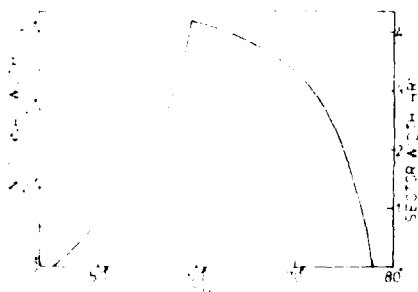


Figure 8. Time Coverage at Different Corrected Geomagnetic Latitudes of the ERS Test Area

For the diurnal motion of the auroral oval, the latitude dependence on the Q index and on the CGLT is computed from Starkov Eq. (1) and is shown in Figure 9. In Figure 9 the abscissa is the corrected geomagnetic local time (CGLT) and the ordinate presents the equatorward boundary of the oval. The curves are for various values of the Q index. From the figure it is seen that ovals with $Q=0, 1$ do not reach the latitude $\lambda=65^\circ$. Even for the highest $Q=9$, the oval is poleward of $\lambda=65^\circ$ for the duration 0815 to 1815 CGLT. Thus even in the case of the strongest magnetic activity $Q=9$ with a continuous duration of 24 hr the oval would reach $\lambda=65^\circ$ only for 14 hr from 1815 to 0815 CGLT. The latitude would be free of auroral disturbance for the remaining 10 hours. This systematic diurnal effect has to be incorporated, so that the probabilities in Table 6 would provide a basis for operational use.

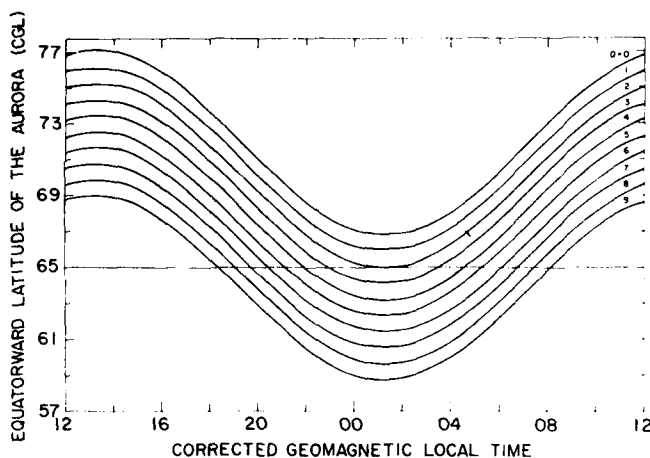


Figure 9. The Diurnal Latitude Dependence of the Auroral Oval for Various Q Values

For operational use, one would seek the probability distributions at various CG latitudes under varying assumptions such as: (a) What is the probability for the auroral oval to affect a specific latitude and longitude?; (b) What is the probability that the whole sector in the test area along a given CG latitude is affected by the auroral oval?; or (c) What is the probability that the auroral oval would affect any section in the test area along a given CG latitude?

Toward achieving this goal, first the general case 'a' of an auroral oval affecting a given latitude and a given longitude will be considered in detail. This will be followed by examples of two selected latitudes for answering the questions

'b' and 'c'. One would then be able to follow/use the procedure for deriving the probabilities for any latitude covered by the ERS test area for satisfying the specific needs like those for 'b' or 'c'.

For the case 'a' the probabilities from corrected Q in Table 2f are combined with the systematic diurnal motion of the auroral oval seen in Figure 9. These probabilities are presented in a series of graphs in Figures 10-1 to 10-18 to cover the CG latitude range of 58° to 75° .

Figure 10-8 is for latitude $\lambda=65^\circ$. A reference to Figure 9 shows that a magnetic disturbance with $Q \geq 2$ is needed for the auroral oval to reach this latitude. A reference to Table 2f shows that the highest cumulative probability (column 2) for $Q \geq 2$ is 68 percent. Thus the highest probability in Figure 10-8, the height of the envelope is 68 percent. Starting from the corrected magnetic local noon, the oval first reaches this latitude at 1645 CGLT and stays (or goes further equatorward) up to 0915 CGLT. During the period 0915 to 1645 CGLT the oval is poleward of, and does not reach the latitude $\lambda=65^\circ$. Also it is recalled that in Figure 9 for the highest value $Q=9$ the duration of the oval at any single longitude and with $\lambda=65^\circ$, is 14 hr (1815 to 0815 CGLT). In Figure 10-8 the maximum duration is (1645 to 0915) 16-1/2 hours. This width is based, in addition, on the distribution of the corrected Q index of 1974. The first curve on the left-hand side in the envelope is for a minimum continuous duration of 15 hr for the disturbance at $\lambda=65^\circ$. The last curve on the right-hand side inside the envelope is for the duration of disturbance to last at least for 1 hr at $\lambda=65^\circ$. For example once the CGLT is 0715 at $\lambda=65^\circ$, the longest duration for this latitude to be affected, cannot be more than 2 hr (from 0715 to 0915 CGLT).

Figure 10-15 presents the expected probabilities at $\lambda=72^\circ$. The Starkov Eq. (1) shows that normal the oval would reach this latitude (from the pole) for 12 hr if $Q=0$. In the figure the 100 percent probability is from 1830 to 0800 CGLT, for a period of 12-1/2 hours. The increased duration arises from the fact that the higher Q values push the oval to lower latitudes ($< 77^\circ$) in the night sector. In the figure, the probability never drops below 42 percent at this latitude. This minimum probability is only for the period from 1100 to 1500 CGLT.

In the above discussion the results are based on the oval boundary determined from discrete auroral arcs from the Starkov equation. An invading aircraft could fly unnoticed under the auroral oval, manifesting a threat over the ERS-area. From the use of graphs in Figure 10, one can predetermine the levels of relative threat at various CG latitudes with time (CGLT) along any given longitude of the ERS test area.

For answering the questions 'b' and 'c' one has to take into account the time widths at respective CG latitudes of the ERS test area. These time widths have already been presented in Figure 8.

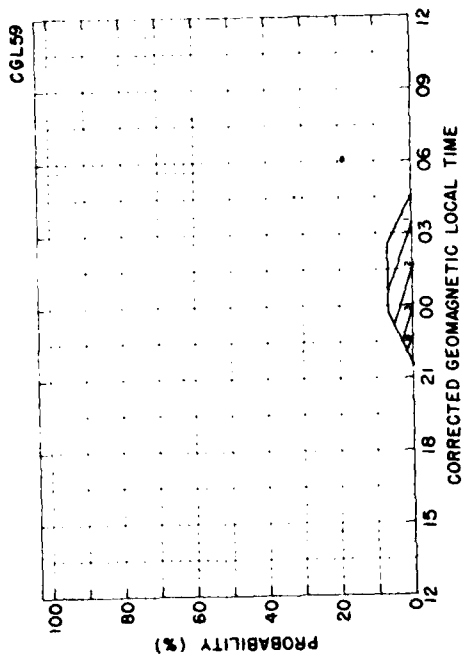


Figure 10-1

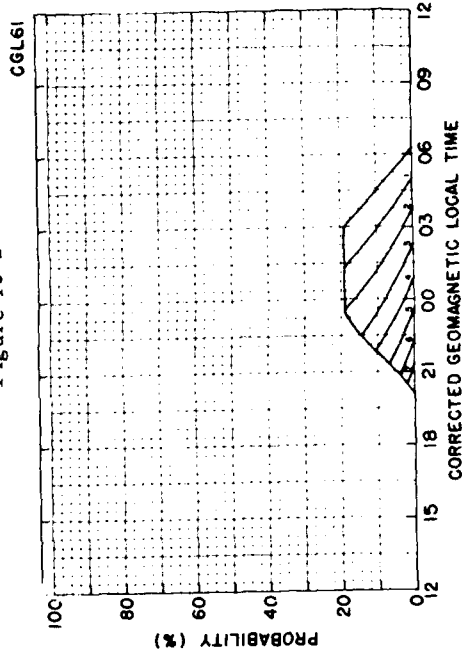


Figure 10-2

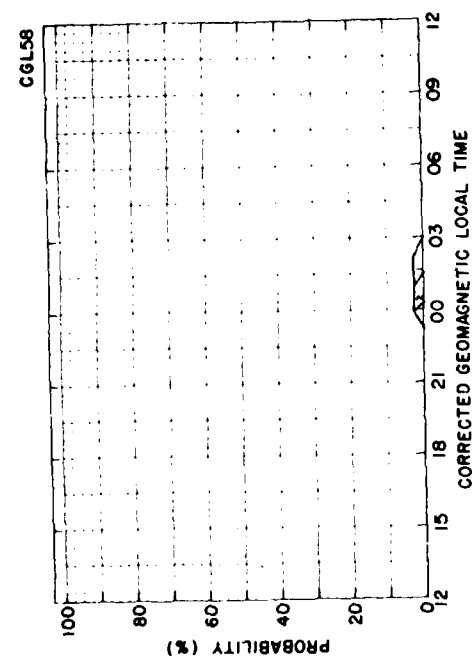


Figure 10-3

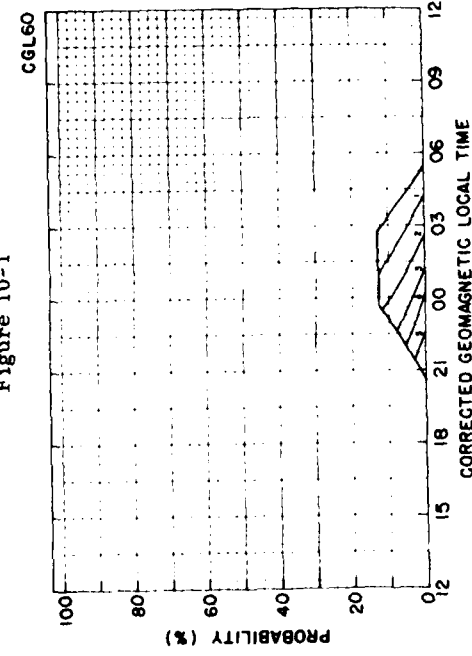
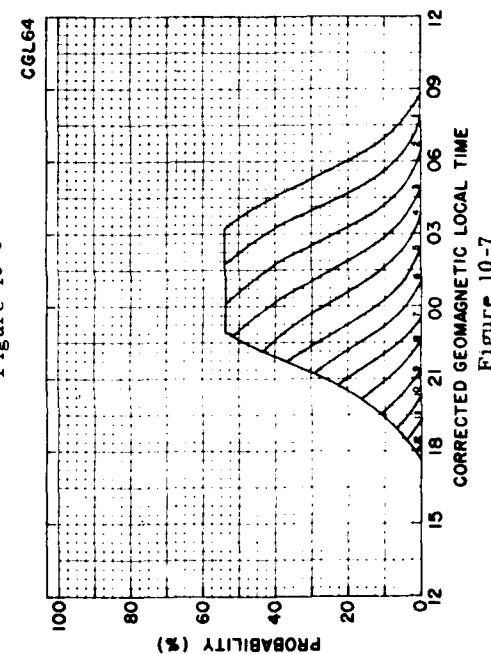
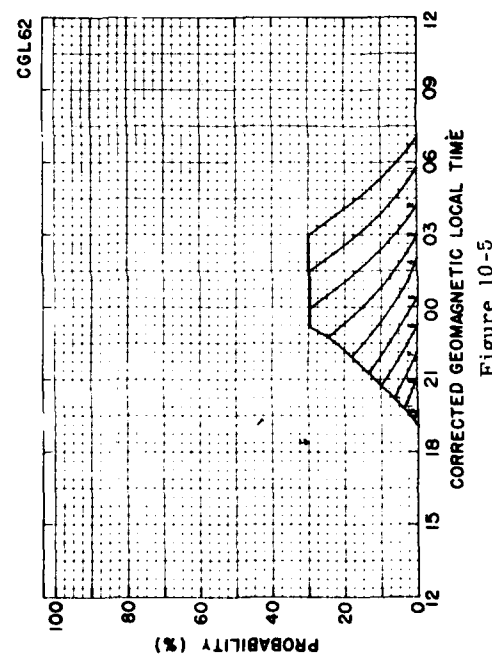
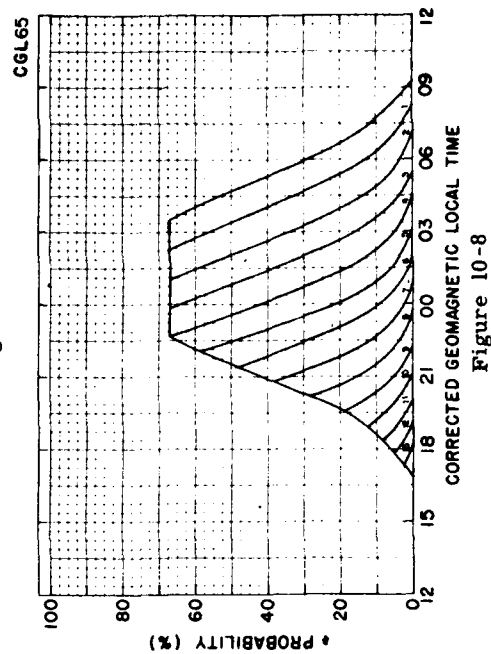
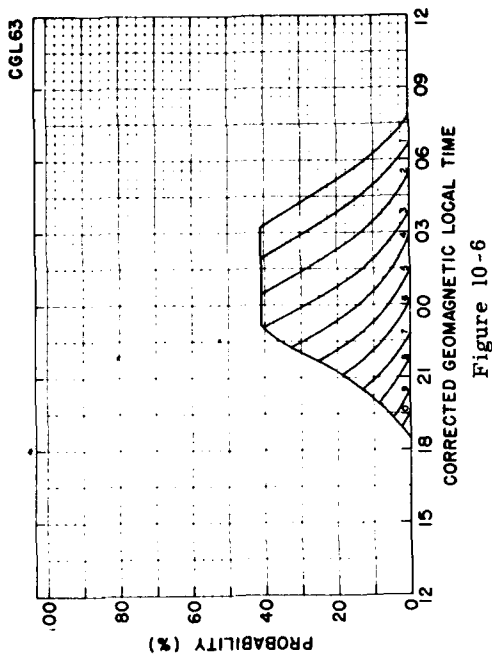


Figure 10-4

Figure 10. Probabilities for Various Durations at a Given CG Latitude and a Single CG Longitude of the ERS Test Area



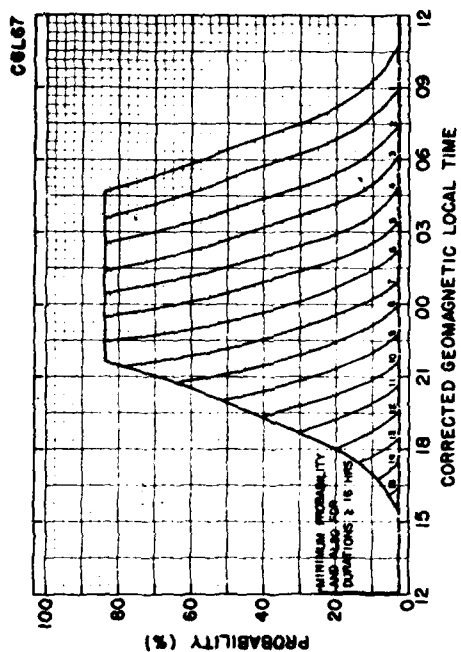


Figure 10-10

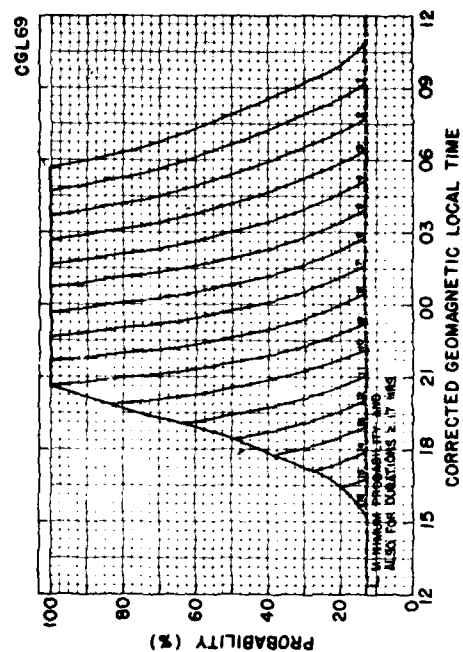


Figure 10-12

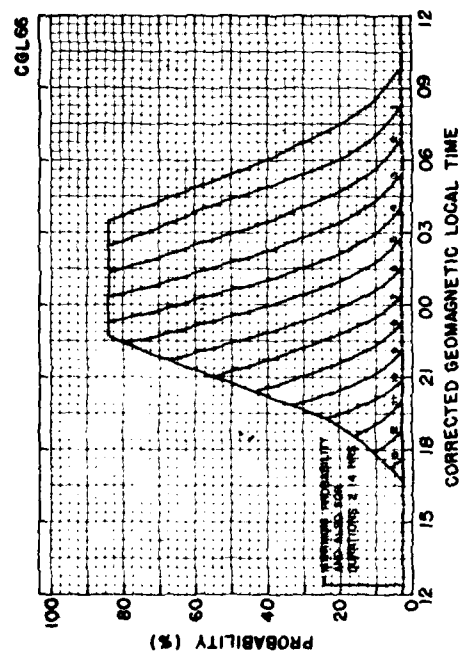


Figure 10-9

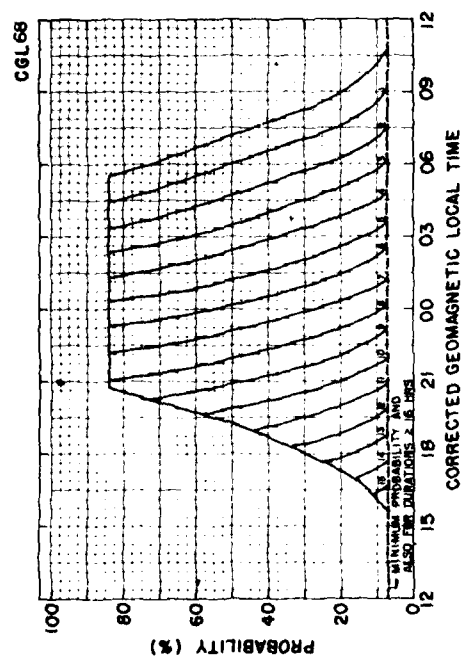


Figure 10-11

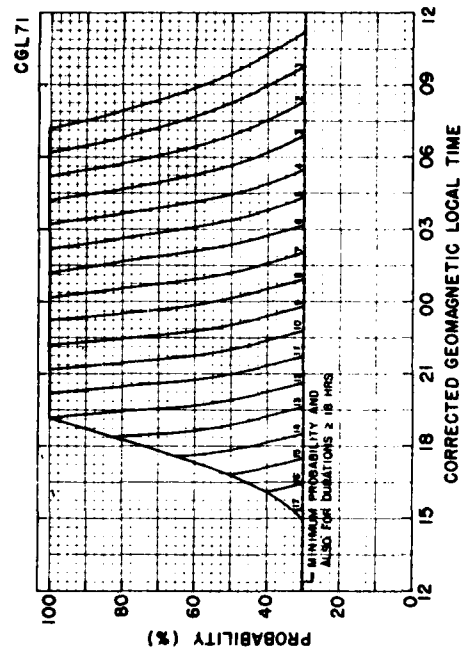


Figure 10-14

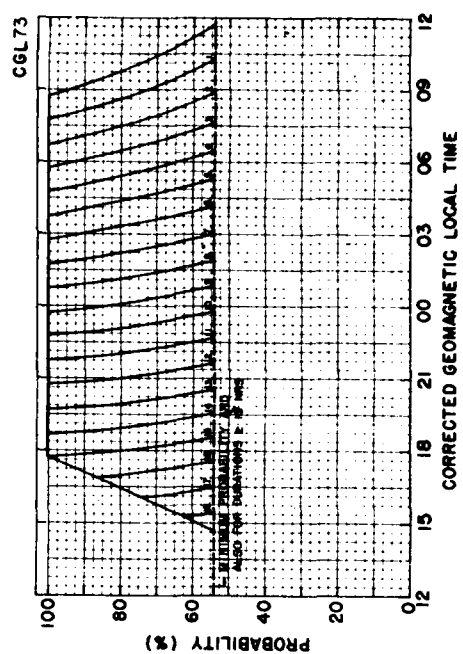


Figure 10-16

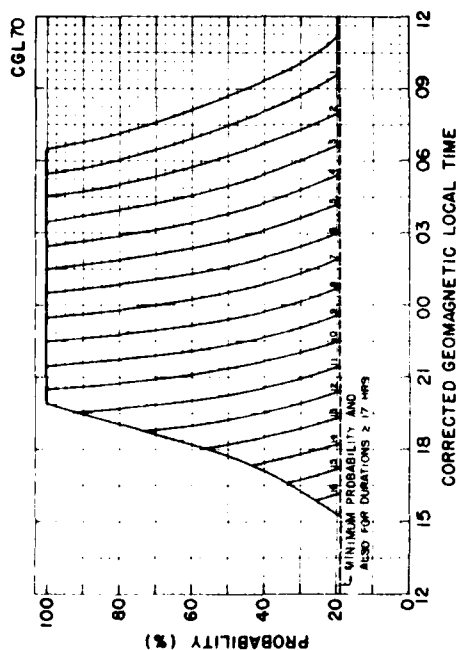


Figure 10-13

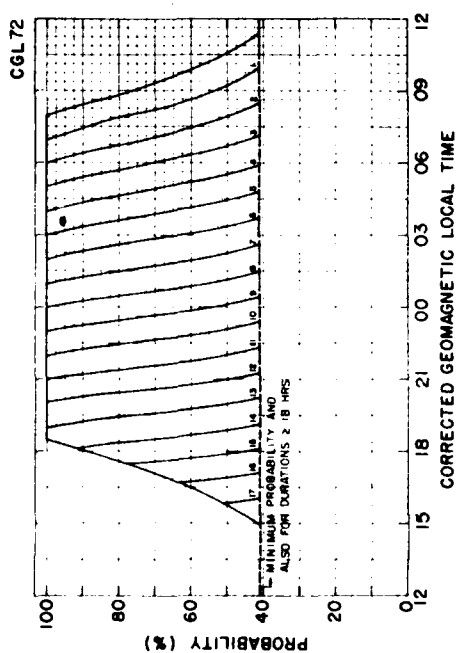


Figure 10-15

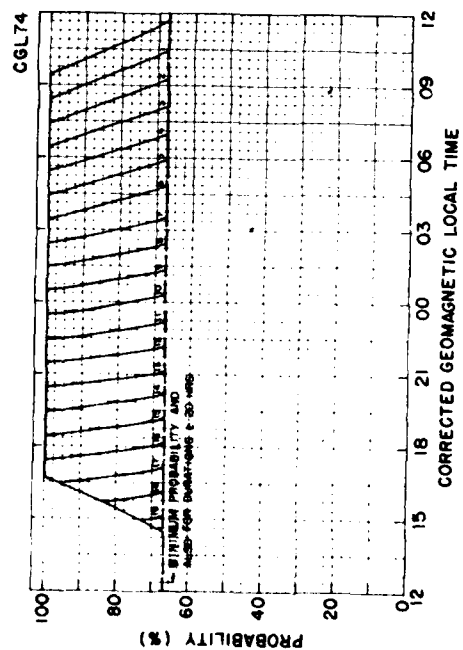


Figure 10-17

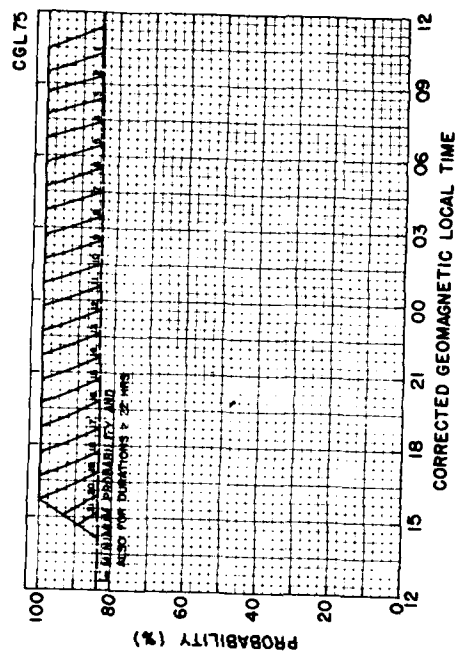


Figure 10-18

When one considers the threat over the entire length along a given CG latitude of the test area, the time intervals are limited such that the auroral oval simultaneously affects both the eastern and the western edges of the test area along that latitude. This additional constraint has to be introduced in the graphs of Figure 10.

Let us consider the situation at $\lambda = 65^\circ$. For the sake of convenience Figure 10-8 is reproduced as Figure 11a1. It is recalled that the graphs in Figure 10 referred to only single longitude. Referring to the ERS test area in Figure 6, the results can be applied to the corrected geomagnetic local time of the western longitude of the ERS test areas, as well as to its eastern longitude. Though the CG Local times are the same for both the western and the eastern edges of the area, the respective local times are separated from each other by 250 min (from Figure 8). When the condition of simultaneous effect at both the ends (east-west) is imposed the time width of the probability curve would reduce (symmetrically) by that amount. The corresponding curves are presented in Figure 11b1. In Figure 11b1 the height of the probability curve, being controlled by the distribution of the corrected Q index, is unchanged. The width of the peak is reduced to 45 min (0045 to 0130) compared to that of 285 min (2245 to 0300) in Figure 11a1. The width at the base 90 percent probability) is reduced correspondingly from 16-1/2 in Figure 11a1 to 12-1/2 hr in Figure 11b1.

Figures 11a2 and 11b2 present results for latitude $\lambda=72^\circ$. The results are similar to those for $\lambda=65^\circ$ in Figures 11a1 and 11b1. In both Figures 11a2 and 11b2, the minimum probability for auroral disturbance is 42 percent. The mere motion of the Starkov oval indicates that the duration should be 12 hr for 100 percent probability due to auroral disturbance at $\lambda=72^\circ$. It is already shown that the Q index distribution increased this duration (Figure 11b1) to 13-1/2 hours. Referring to Figure 8, the time width of the ERS test area at $\lambda=72^\circ$ is 180 minutes. This reduces the width of simultaneous effect over the test area at $\lambda=72^\circ$ by 3 hr from Figure 11a2 to Figure 11b2.

In answering question 'c' it follows that one would have to extend the time width such that, even if one edge (eastern/western) is clear of any auroral disturbances, the possibility that the remaining edge of the test area could be affected, has to be considered. Thus the widths of the graphs in Figure 10 have to be increased to take into account the time width of the ERS test area at various latitudes already shown in Figure 8. The corresponding results are presented in Figures 11c1 and 11c2 for latitudes 65° and 72° respectively. In contrast to the reduction in widths from Figures 11a1 and 11a2 to Figures 11b1 and 11b2, one now sees an increase in the widths by the same amounts in the respective Figures 11c1 and 11c2 (from Figures 11a1 and 11a2).

Thus one can select and/or derive a set of graphs from Figure 10, to satisfy the specific needs different from those of the operational use of the graphs in Figure 10.

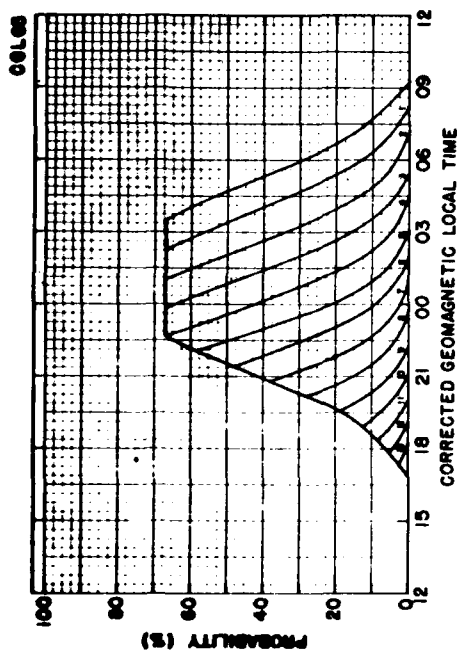


Figure 11a1. Copy of Figure 10-8

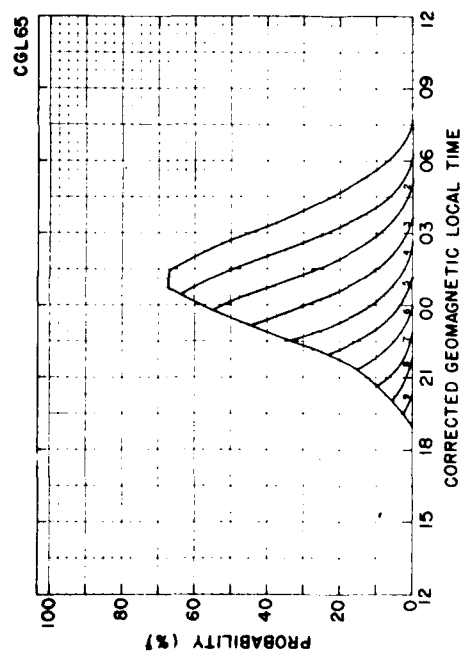


Figure 11b1. Probability That the Entire ERS Test Area at $\lambda=65^\circ$ Would be Affected by the Auroral Oval

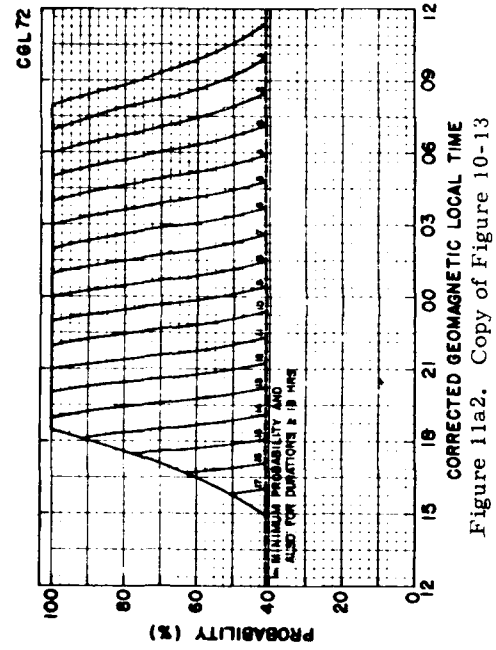


Figure 11a2. Copy of Figure 10-13

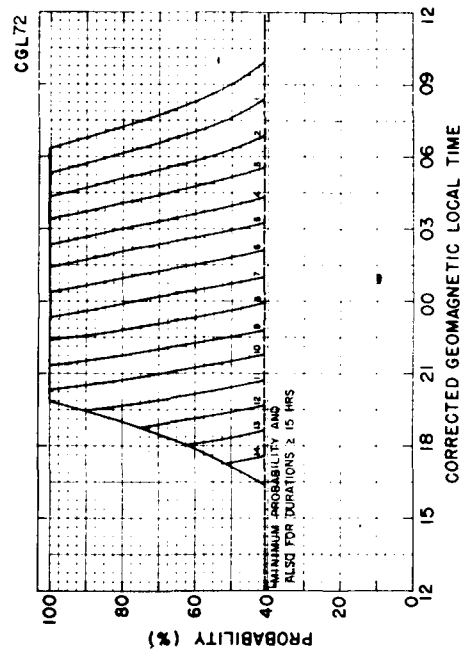


Figure 11b2. Similar to That of Figure 11b1 for $\lambda=72^\circ$

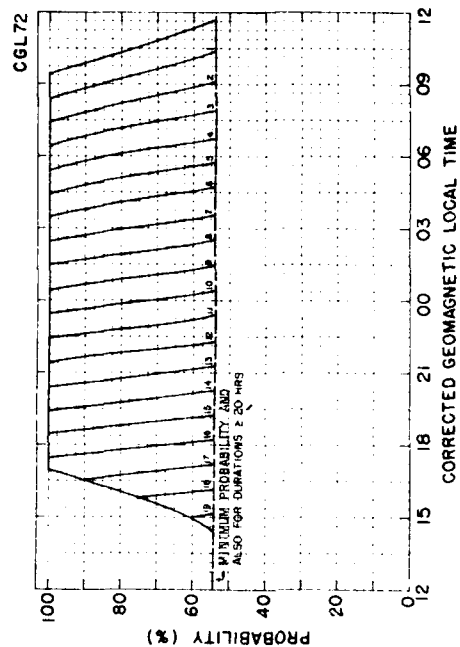


Figure 11c2. Similar to That of Figure 11c1 for $\lambda=72^\circ$

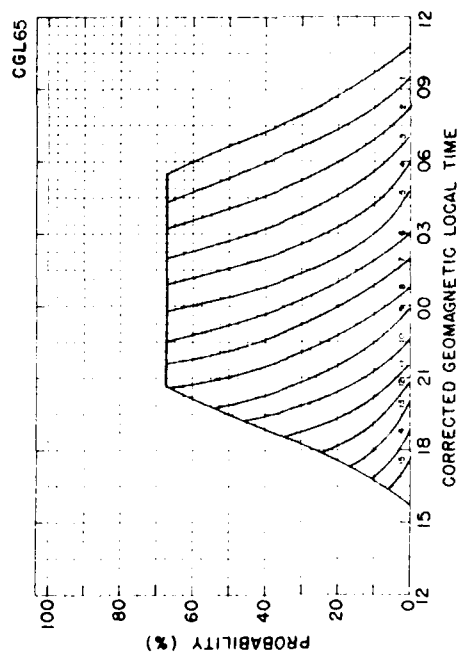


Figure 11c1. Probability That Any Point in the ERS Test Area at $\lambda=65^\circ$ Would be Affected by the Auroral Oval

4. CONCLUSIONS

The presence of one or more phenomena such as discrete aurora, continuous (diffuse) aurora, sporadic E layer E_s , auroral E layer E_a , F_2 layer, F layer irregularity zone (FLIZ), the ionospheric trough, could affect the test area. Depending on the factors such as the locations of the transmitter and the receiver of the radar system, the emission power of the transmitter, the threshold signal detectability of the receiver, one has to determine as to which of the above phenomena, the radar system is most susceptible.

The statistical study of the Q index data in 1974 from Sodankyla, in conjunction with the ERS test area, shows that only about one-fourth of the poleward sector of the area is affected by auroral disturbances for more than 50 percent of the time. The middle one-third portion is affected for less than 25 percent of the time and the bottom third portion is free of any auroral disturbances at all times.

In all the above discussion, the location of the equatorward boundary of discrete auroral arcs from the Starkov equation, was the criterion affecting the regions in the test area. For example, if instead, the radar system is susceptible to diffuse aurora, in preference to discrete auroral arcs, another study⁴ has shown, that the diffuse aurora statistically lie 3° equatorwards of the discrete arcs. Thus the probabilities presented in Tables 5 and 6 at various latitudes have to be moved 3° equatorwards. Thus the present probability at 75° CGL from discrete auroral arcs has to be used for 72° CGL in case of diffuse aurora.

This report has developed a technique to determine the effect of the variation of the Q index measured from a single auroral station on the radio wave surveillance in the coverage area of a OTH backscatter radar system. To facilitate this demonstration a number of illustrations and tables have been presented. This will ease the application of this technique to any other test area covered by any radar system.

The first section shows that the Q index measured from a single auroral station exhibits a diurnal variation due to the movement of the earth under an auroral oval. This systematic diurnal variation can be eliminated effectively by determining a set of empirical factors. The corrected data set from a single station may then be used reliably for computing the durations as well as the levels of magnetic (and auroral) disturbances.

The second section combines the location of the auroral oval at various CG latitudes expected from the Starkov equation, with the corrected durations and corrected levels of the magnetic activity index Q, for obtaining the probabilities

4. Dandekar, B.S. (1979) Study of the Equatorward Edge of the Auroral Oval from Satellite Observations, AFGL-TR-79-0010, AD A072997.

for the disturbances on a global base. These probabilities are smaller for a location at any single selected longitude. The values for probabilities for a test area with a definite longitudinal width lie between these two extremes (of Tables 5 and 6).

In the OTH-B ERS coverage area the window varies with the locations along the CG latitudes as shown in Figure 9. For operational usage the combined effect of the time width of the ERS test area at various latitudes, the systematic diurnal motion of the oval and a priori distribution of the corrected Q index (1974) is taken into account. The final results for practical use are presented as a series of graphs (Figures 10-1 through 10-13) for various latitudes.

This detailed step-by-step presentation should enable one to use the Q index data over any period for determining the expected probabilities of auroral disturbances for different levels and durations of magnetic activity for any test area to be under surveillance.